Room-Temperature Tunnel Magnetoresistance and Spin-Polarized Tunneling through an Organic Semiconductor Barrier

T. S. Santos,[1] J. S. Lee,[1,2] P. Migdal,[1] I. C. Lekshmi,[1] B. Satpati,[3] and J. S. Moodera[1]

[1]*Francis Bitter Magnet Laboratory, Massachusetts Institute of Technology, Cambridge, Massachusetts 02139, USA*

[2]*Nano-device Research Center, Korea Institute of Science and Technology, Seoul, Korea*

[3]*Paul Drude Institute for Solid State Electronics, Berlin, Germany*

(Received 4 August 2006; published 5 January 2007)

Electron spin-polarized tunneling is observed through an ultrathin layer of the molecular organic semiconductor tris(8-hydroxyquinolinato)aluminum (Alq_3). Significant tunnel magnetoresistance (TMR) was measured in a $Co/Al_2O_3/Alq_3/NiFe$ magnetic tunnel junction at room temperature, which increased when cooled to low temperatures. Tunneling characteristics, such as the current-voltage behavior and temperature and bias dependence of the TMR, show the good quality of the organic tunnel barrier. Spin polarization (P) of the tunnel current through the Alq_3 layer, directly measured using superconducting Al as the spin detector, shows that minimizing formation of an interfacial dipole layer between the metal electrode and organic barrier significantly improves spin transport.

DOI: 10.1103/PhysRevLett.98.016601 PACS numbers: 72.25.Dc, 72.80.Le, 75.47.−m, 85.75.−d

There is considerable activity of late in the field of organic electronics from the fundamental physics point of view as well as with the promise of developing cheaper and flexible devices, such as organic light-emitting diodes (OLEDs) and organic transistors. While these materials are exploited for their tunability of charge-carrier transport properties, their *spin* transport properties is a least explored area, especially for organic semiconductors (OSCs), which are pertinent for future spin-based electronics. Because OSCs are composed of mostly light elements (i.e., C, H, N, or O) and thus have a weaker spin-orbit interaction compared to inorganic semiconductors, spin coherence lengths can be long in these materials. Recent observations of magnetoresistance (MR) effects in OSCs has opened up the potential of these materials for spin-conserved transport. In an organic spin valve study using Alq_3 as the spacer layer between ferromagnetic $La_{0.67}Sr_{0.33}MnO_3$ (LSMO) and Co electrodes, Xiong *et al.* [1] measured a giant inverse magnetoresistance (GMR) of 40% at 11 K, which reduced to zero by $T > 200$ K. The thickness range of Alq_3 used in that study was from 130 to 260 nm, and a spin diffusion length of 45 nm was estimated at liquid helium temperatures. They also concluded that there was an ill-defined layer of ~100 nm of Alq_3 containing Co inclusions. Mermer *et al.* [2] showed room-temperature MR of polyfluorene films and Alq_3 films several nanometers thick, sandwiched between *nonferromagnetic* electrodes. Utilizing the Alq_3 molecule at the monolayer level, we demonstrate spin-polarized tunneling through an OSC at room temperature and the effect of interfacial charge states on spin injection. This study opens up the possibility for many future investigations in this area, which is expected to be rich in physics as well as device potential.

The organic π-conjugated molecular semiconductor Alq_3 ($C_{27}H_{18}N_3O_3Al$) is the most widely used electron transporting and light-emitting material in OLEDs. Alq_3 has been extensively studied for this application since it displayed high electroluminescence (EL) efficiency nearly two decades ago [3]. A band gap of 2.8 eV separates the highest occupied molecular orbital and the lowest unoccupied molecular orbital. Typically, the film thickness of the Alq_3 layers in OLEDs and structures for MR studies is tens to hundreds of nanometers. In the present study, we have successfully fabricated Alq_3 films <2 nm thick as a tunnel barrier between two ferromagnetic electrodes. The resistance of this magnetic tunnel junction (MTJ) depends on the relative orientation of the magnetization of the two ferromagnets (FMs): lower resistance for parallel alignment (R_P) and higher resistance for antiparallel alignment (R_{AP}) [4,5]. Tunnel magnetoresistance (TMR) is defined as $\Delta R/R = (R_{AP} - R_P)/R_P$, and has a positive value for our MTJs with the Alq_3 barrier, even at room temperature. To further corroborate the positive TMR found in this study, we also performed a direct measurement of P for the tunnel current from several FMs through the Alq_3 barrier, by utilizing superconducting Al as the spin detector.

Tunnel junctions were prepared *in situ* in a high vacuum deposition chamber with a base pressure of 6×10^{-8} Torr. The MTJs were deposited on glass substrates at room temperature having the structure, listed in the order of deposition, 1 nm SiO/8 nm $Co/Al_2O_3/Alq_3$/10 nm $Ni_{80}Fe_{20}$. The Co and $Ni_{80}Fe_{20}$ [permalloy (Py)] electrodes were patterned by shadow masks into a cross configuration. The Alq_3 tunnel barrier was grown by thermal evaporation from a Alq_3 powder source at a rate of ~0.3 nm/s. Junctions with six different Alq_3 thicknesses, from 1 to 4 nm, were prepared in a single run by using a rotating sector disk. A thin Al_2O_3 layer of ~0.6 nm at the interface between the Co electrode and the Alq_3 barrier was formed by depositing Al film and then oxidizing it by a short exposure (~2 s) to oxygen plasma. Film thickness was

monitored *in situ* by a quartz crystal oscillator, and the density of Alq_3 used was 1.5 g/cm^3 [6]. Tunnel junctions for direct measurement of P were made, similarly having the structure 3.8 nm Al/Alq_3/8 nm Co or Fe or Py, with and without an ultrathin layer of Al_2O_3 at the Al/Alq_3 interface. The junction area was 200×200 μm^2.

Growth of the Alq_3 films was uniform and continuous, as shown by the cross-sectional high-resolution transmission electron microscope (HRTEM) image of thin Alq_3 between Co and Py. X-ray diffraction of the Alq_3 films >50 nm thick showed the amorphous structure of the film. No change in the chemical structure of Alq_3 is expected during thermal deposition in vacuum [7], and the monolayer thickness of Alq_3 is ~1 nm [8]. Alq_3 films at the monolayer level on metal and Al_2O_3 underlayers have been well studied earlier [7–11].

Junction resistance (R_J) was measured using a four-point probe configuration. The tunneling characteristics were measured for 4 sets of MTJs, with 72 junctions per set, and the results were consistent. In a given junction preparation run with six different Alq_3 thicknesses, R_J scaled exponentially with Alq_3 thickness (see inset of Fig. 1), which shows that tunneling is occurring through the Alq_3 layer [12]. This observation, combined with TEM data, rules out the possibility that the Alq_3 layer was discontinuous and only acted to reduce the effective junction area for direct tunneling through the Al_2O_3 layer. If the latter were the case, because $R_J \propto$ (junction area)$^{-1}$, the R_J dependence on Alq_3 thickness would follow the dashed line shown in Fig. 1 inset. Upon cooling from room temperature down to 4.2 K, R_J rose by a factor of 2 to 3 [see inset of Fig. 2(a)]. Such increase in R_J with decreasing temperature is common for junctions with semiconductor tunnel barriers [13], as opposed to pure, insulating Al_2O_3 barriers which show a R_J increase of ~20% between 300 and 1.2 K.

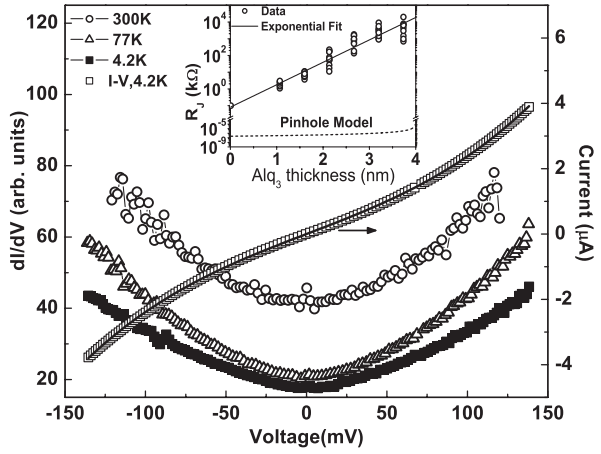

FIG. 1. *I-V* characteristics for an 8 nm Co/0.6 nm Al_2O_3/1.6 nm Alq_3/10 nm Py junction. The fit of the *I-V* curve to BDR's equation is also shown (line). The inset shows the exponential dependence of R_J on Alq_3 thickness, for a total of 72 junctions made in a single run.

The current-voltage (*I-V*) characteristics for one MTJ are shown in Fig. 1 and are representative of all MTJs measured. The *I-V* curve was fit using the model of Brinkman, Dynes, and Rowell (BDR) [14], yielding values of 0.47 eV for tunnel barrier height (Φ), 0.01 eV for barrier asymmetry ($\Delta\Phi$), and 3.3 nm for barrier thickness (s). Given an uncertainty in actual barrier thickness and the large size of the Alq_3 molecule, a value of $s = 3.3$ nm found from the fit is nominal. The Φ value of 0.47 eV is reasonable for Alq_3, which has a band gap of 2.8 eV [15]. As shown in Fig. 1, the shape of the conductance (dI/dV) versus bias is similar at room temperature and low temperatures, only shifted down due to the higher R_J at lower temperatures. It is necessary to note the absence of a sharp dip at zero bias (known as the zero bias anomaly), especially for lower temperatures. This shows that the barrier and interfaces are free of magnetic inclusions. The presence of such a dip in conductance can be caused by diffusion of magnetic impurities into the barrier, among other possibilities [16]. In the double barrier structure, with Al_2O_3 and Alq_3, dI/dV versus V at all temperatures is symmetric with no offset present, signifying a rectangular

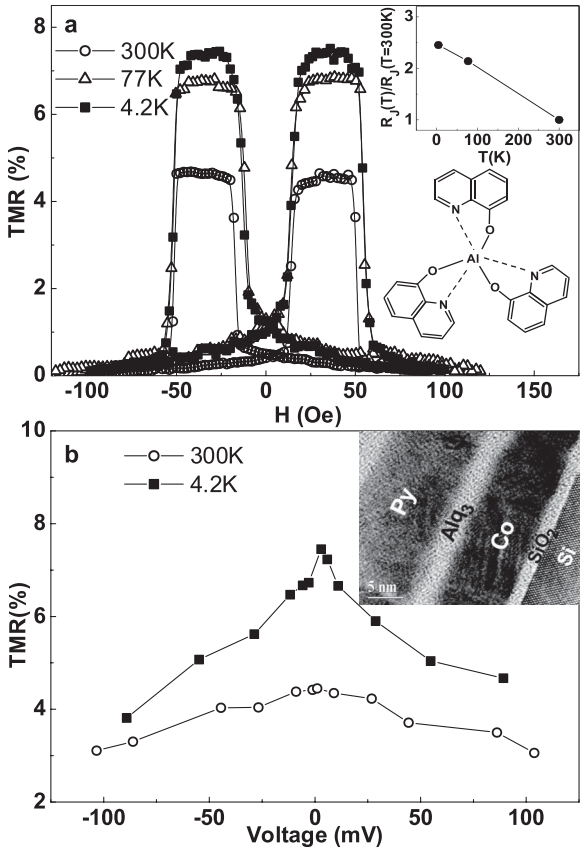

FIG. 2. TMR for an 8 nm Co/0.6 nm Al_2O_3/1.6 nm Alq_3/10 nm Py junction. (a) TMR measured with 10 mV bias. The inset shows the temperature dependence of R_J for this junction and the chemical structure of the Alq_3 molecule. (b) Bias dependence of the TMR. The inset is a cross-sectional HRTEM image of a MTJ, showing the continuous Alq_3 barrier.

potential barrier [12]. This symmetric barrier is reasonable when considering the low barrier height for ultrathin Al_2O_3 [17] and the amorphous structure of both Al_2O_3 and Alq_3 [13]. The junctions are stable up to an applied bias of $\sim \pm 150$ mV and show properties that are reproducible over time. These properties—the exponential thickness dependence of R_J, strong temperature dependence of R_J, and nonlinear I-V, along with the TEM data—confirm that tunneling is occurring through the Alq_3 layer, rather than singly through pinholes and the Al_2O_3 layer. Thus, these organic barrier MTJs show good tunneling behavior.

TMR for an 8 nm Co/0.6 nm Al_2O_3/1.6 nm Alq_3/10 nm Py junction measured with a 10 mV bias is shown in Fig. 2(a), with TMR values of 4.6%, 6.8%, and 7.5% at 300, 77, and 4.2 K, respectively. Well-separated coercivities of the Co and Py electrodes yield well-defined parallel and antiparallel magnetization alignment, clearly showing the low resistance (R_P) and high resistance (R_{AP}) states, respectively. Similar TMR values and temperature dependence was observed for all Alq_3 barrier junctions. The highest TMR value seen at 300 K was 6.0%.

The bias dependence of the TMR for the same junction at 300 and 4.2 K is shown in Fig. 2(b) and is symmetric for $\pm V$. Substantial TMR persists even beyond ± 100 mV. A decrease of TMR with increasing bias voltage has been observed for even the best quality MTJs with Al_2O_3 barriers, and is attributed to the excitation of magnons, phonons, band effects, etc., at higher voltages [18]. In addition, for the present junctions with the Alq_3 barrier, one can expect chemistry-induced states in the Alq_3 band gap [10] (discussed below), which would give rise to increased temperature and bias dependence as well as reduced TMR [19].

To directly determine P for the tunnel current from Co, Fe, and Py electrodes through the Alq_3 barrier, junctions with an Al counterelectrode were cooled to 0.4 K in a He^3 cryostat and dI/dV versus bias was measured. Shown in Fig. 3 is dI/dV of a 3.8 nm Al/Al_2O_3/1.5 nm Alq_3/8 nm Co junction and a 3.7 nm Al/3.7 nm Alq_3/3 nm Co/6 nm Py junction, displaying the characteristic behavior of conduction by tunneling into a superconductor [20]. The Al electrode was superconducting below $\sim$2.9 K. Negligible leakage at $V = 0$ and the sharp peaks at the superconducting gap voltage, seen in the zero field conductance curve, confirms the high quality of the Alq_3 tunnel barrier without any Co inclusions.

When a magnetic field (H) is applied in the plane of the film, Zeeman splitting of the conductance peaks is observed with magnitude $2\mu_B H$. Asymmetry of the conductance, seen here, is the classic signature for polarization of the tunnel current [20]. To extract P, the dI/dV curve was fit with Maki's theory, taking into account orbital depairing and spin-orbit scattering [21]. For the Co electrode and Al_2O_3/Alq_3 barrier, a P value of 27% was determined. Similarly, P values of 30% for Fe and 38% for Py were determined. This measurement clearly demonstrates polarization of the tunnel current from a FM through an OSC.

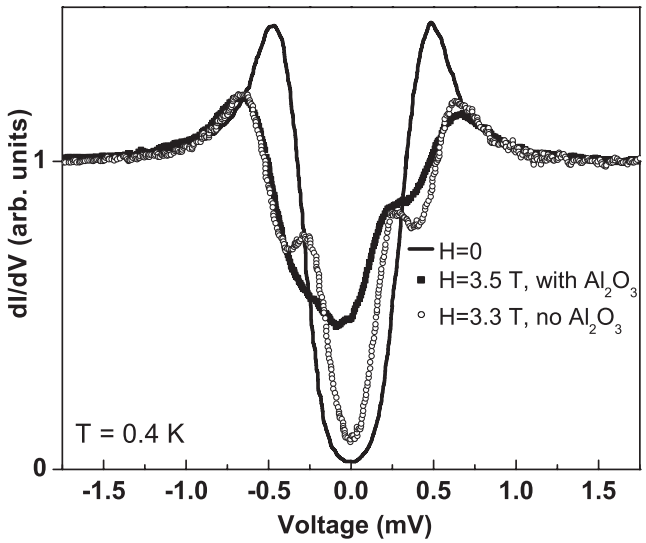

FIG. 3. Conductance of a 3.8 nm Al/Al_2O_3/1.5 nm Alq_3/8 nm Co junction (solid squares) and a 3.7 nm Al/3.7 nm Alq_3/3 nm Co/6 nm Py junction (open circles), with and without an applied magnetic field. Zero field curves for both junctions were nearly identical; only one is shown for clarity.

However, the value of P was down to 6% for the junction without Al_2O_3 at the Al/Alq_3 interface, as shown in Fig. 3. BDR fitting of the I-V curve for the junction with a Al_2O_3/Alq_3 barrier yielded values of $\Phi = 0.52$ eV, $\Delta\Phi \sim 0$, and $s = 3.1$ nm, which are in good agreement with those of the MTJs (Fig. 1). The corresponding parameters for the junction with a pure Alq_3 barrier were $\Phi = 1.8$ eV, $\Delta\Phi \sim 0$, and $s = 1.6$ nm.

For both junction structures, with and without Al_2O_3 at the Al/Alq_3 interface, we measured positive P for Co, Fe, and Py electrodes, which is in agreement with the positive TMR we measured. This is in contrast to the inverse GMR observed by Xiong *et al.* in a LSMO/Alq_3/Co spin valve [1]. This discrepancy can be attributed to the different conduction mechanisms responsible for the GMR and TMR effects [22]. Contrary to the speculation of Xiong *et al.* based on tunneling that their inverse GMR is due to the negative polarization of the Co d band at the Fermi level, inverse GMR may originate from the opposite spin asymmetry coefficients of Co and LSMO, as shown by Vouille *et al.* [23]. Also, the role of Co inclusions (to a depth of $\sim$100 nm in the Alq_3) on the observed inverse GMR is unclear. The tunneling behavior observed in our study is similar to that of both amorphous Al_2O_3 and amorphous $SrTiO_3$ tunnel barriers [24], in which positively polarized, itinerant sp electrons dominate spin transport [25].

The high barrier height for the junction with a pure Alq_3 barrier in Fig. 3 can be attributed to a dipole layer formed at the metal-Alq_3 interface. Such a phenomenon has previously been observed in tunnel junctions with a layer of organic material adsorbed at the barrier interface [14,26].

This dipole barrier is also present at the metal-organic interface in OLEDs [27] and has been attributed to charge transfer, chemical reactions, and changes of molecular configuration, which introduce states into the Alq_3 band gap [10]. These intrinsic gap states are concentrated mainly at the metal-organic interface. Thus, the bulk of the Alq_3 film is a good quality tunnel barrier, producing a conductance with negligible leakage current (Fig. 3). Yet the presence of the gap states manifest themselves in the reduced P value and more noise in the dI/dV measurement, compared to the junction with an Al_2O_3 interfacial layer. The charge states appear to localize the tunneling spins, thereby reducing spin-conserved tunneling [28]. It is known from OLED studies that a very thin layer ($\sim$1 nm) of Al_2O_3 at the cathode-Alq_3 interface suppresses the formation of these gap states and effectively lowers the barrier height to electron injection via tunneling across the interface, resulting in more efficient injection and enhanced EL output [9,29]. Likewise, the ultrathin Al_2O_3 layer at the electrode-Alq_3 interface of our tunnel junctions results in significantly higher P, lower Φ, and less noise in the dI/dV measurement. This result demonstrates the degrading effect of interfacial charge states in spin-conserved tunneling and how minimizing formation of these states greatly improves spin injection efficiency across the FM/OSC interface. Finally, MTJs prepared with pure Alq_3 barriers up to 20 nm thick were unstable and did not show good tunneling behavior, likely caused by the chemical nature of the Co/Alq interface [11], leading to multistep conduction via these gap states.

In summary, we have observed TMR at room temperature in MTJs with an OSC barrier. P of the tunnel current through the OSC is directly measured using a superconductor as the spin detector. This work shows that spin-conserved transport through organic systems is possible, which can lead to the development of spin-based molecular electronics.

The authors thank P. LeClair for his help and G. X. Miao and E. Tsymbal for useful discussions. This work is funded by NSF grants, an ONR grant, and partially by the KIST-MIT program.

[1] Z. H. Xiong, D. Wu, Z. V. Vardeny, and J. Shi, Nature (London) **427**, 821 (2004).
[2] Ö. Mermer, G. Verraraghavan, T. L. Francis, Y. Sheng, D. T. Nguyen, M. Wohlgenannt, A. Köhler, M. K. Al-Suti, and M. S. Khan, Phys. Rev. B **72**, 205202 (2005).
[3] C. W. Tang and S. A. VanSlyke, Appl. Phys. Lett. **51**, 913 (1987).
[4] M. Julliere, Phys. Lett. **54A**, 225 (1975).
[5] J. S. Moodera, L. R. Kinder, T. M. Wong, and R. Meservey, Phys. Rev. Lett. **74**, 3273 (1995).
[6] C. H. M. Marée, R. A. Weller, L. C. Feldman, K. Pakbaz, and H. W. H. Lee, J. Appl. Phys. **84**, 4013 (1998).
[7] T. Gavrilko, R. Fedorovich, G. Dovbeshko, A. Marchenko, A. Naumovets, V. Nechytaylo, G. Puchkovska, L. Viduta, J. Baran, and H. Ratajczak, J. Mol. Struct. **704**, 163 (2004).
[8] X. M. Ding, L. M. Hung, C. S. Lee, and S. T. Lee, Phys. Rev. B **60**, 13 291 (1999).
[9] K. L. Wang, B. Lai, M. Lu, X. Zhou, L. S. Liao, X. M. Ding, X. Y. Hou, and S. T. Lee, Thin Solid Films **363**, 178 (2000).
[10] C. Shen, A. Kahn, and J. Schwartz, J. Appl. Phys. **89**, 449 (2001).
[11] A. N. Caruso, D. L. Schulz, and P. A. Dowben, Chem. Phys. Lett. **413**, 321 (2005).
[12] J. G. Simmons, J. Appl. Phys. **34**, 1793 (1963).
[13] G. A. Gibson and R. Meservey, J. Appl. Phys. **58**, 1584 (1985).
[14] W. F. Brinkman, R. C. Dynes, and J. M. Rowell, J. Appl. Phys. **41**, 1915 (1970).
[15] *Tunnel Spectroscopy*, edited by P. K. Hansma (Plenum Press, New York, 1982).
[16] J. Appelbaum, Phys. Rev. Lett. **17**, 91 (1966).
[17] B. Oliver and J. Nowak, J. Appl. Phys. **95**, 546 (2004).
[18] J. S. Moodera, J. Nowak, and R. J. M. van de Veerdonk, Phys. Rev. Lett. **80**, 2941 (1998).
[19] J. S. Moodera and G. Mathon, J. Magn. Magn. Mater. **200**, 248 (1999).
[20] R. Meservey and P. M. Tedrow, Phys. Rep. **238**, 173 (1994).
[21] K. Maki, Prog. Theor. Phys. **32**, 29 (1964).
[22] P. M. Levy and I. Mertig, in *Spin Dependent Transport in Magnetic Nanostructures*, edited by S. Maekawa and T. Shinjo, Advances in Condensed Matter Science (Taylor & Francis, London, 2002), Chap. 2, pp. 47–111.
[23] C. Vouille, A. Barthélémy, F. Elokan Mpondo, A. Fert, P. A. Schroeder, S. Y. Hsu, A. Reilly, and R. Loloee, Phys. Rev. B **60**, 6710 (1999).
[24] A. Thomas, J. S. Moodera, and B. Satpati, J. Appl. Phys. **97**, 10C908 (1999).
[25] M. B. Stearns, J. Magn. Magn. Mater. **5**, 167 (1977); M. Münzenberg and J. S. Moodera, Phys. Rev. B **70**, 060402(R) (2004).
[26] D. G. Walmsley, R. B. Floyd, and W. E. Timms, Solid State Commun. **22**, 497 (1977).
[27] I. G. Hill, A. Rajagopal, A. Kahn, and Y. Hu, Appl. Phys. Lett. **73**, 662 (1998); S. T. Lee, X. Y. Hou, M. G. Mason, and C. W. Tang, Appl. Phys. Lett. **72**, 1593 (1998).
[28] R. Jansen and J. S. Moodera, Phys. Rev. B **61**, 9047 (2000).
[29] F. Li, H. Tang, J. Anderegg, and J. Shinar, Appl. Phys. Lett. **70**, 1233 (1997).